Article

# Selective Hydrogenation of Unsaturated Carbon-Carbon Bonds in Aromatic-Containing Platform Molecules

Thomas J. Schwartz, Spencer D. Lyman, Ali Hussain Motagamwala , Max A. Mellmer, and James A. Dumesic

*ACS Catal.*, **Just Accepted Manuscript** • DOI: 10.1021/acscatal.6b00072 • Publication Date (Web): 12 Feb 2016



ACS Catalysis is published by the American Chemical Society. 1155 Sixteenth Street N.W., Washington, DC 20036

# Selective Hydrogenation of Unsaturated Carbon-Carbon Bonds in Aromatic-Containing Platform Molecules

*Thomas J. Schwartz,*[†] *Spencer D. Lyman, Ali Hussain Motagamwala, Max A. Mellmer, James A. Dumesic*[*]

Department of Chemical and Biological Engineering, University of Wisconsin–Madison, Madison, WI 53706

ABSTRACT

The combination of chemical and biological catalysis enables the production from biomass of coumarin and dihydrocoumarin (DHC), opening new routes to the formation of fine chemicals and pharmaceutical building blocks. Each of these products requires the hydrogenation of 4-hydroxycoumarin (4HC) to 4-hydroxydihydrocoumarin (4HDHC), which in turn requires the reduction of an unsaturated carbon-carbon bond in the presence of an aromatic ring. Using *in situ* attenuated total reflection Fourier transform infrared (ATR-FTIR) spectroscopy, we show that reaction at 348 K over monometallic Pd catalysts leads to the partial reduction of the aromatic ring in 4HC, obtaining 93% selectivity for C=C bond hydrogenation at 82% 4HC conversion and with a low turnover frequency (TOF). Decreasing the Pd dispersion from 70% to

6% not only leads to an increase in the rate of 4HC hydrogenation, but it also leads to an increase in the rate of over-hydrogenation. However, the formation of bimetallic PdAu nanoparticles inhibits the over-hydrogenation reaction while also doubling the TOF to a value of 6 $ks^{-1}$ for 4HDHC production. A bimetallic PdAu catalyst supported on $SiO_2$ leads to 97% selectivity for C=C bond hydrogenation at 86% 4HC conversion, while an acidic support such as amorphous silica-alumina can be used to produce DHC directly from 4HC.

KEYWORDS. Selective Hydrogenation, Bimetallic Catalysts, Heterogeneous Catalysis, Biocatalysis, Biorenewable Chemicals, Fine Chemicals

## 1. INTRODUCTION

Shifts in the price and availability of fossil-based feedstocks for the production of fuels and chemicals have led to research in the use of biomass as a renewable source of carbon and the emergence of nascent biofuels and biorenewable chemicals industries.[1] While recent advances in the recovery of shale gas and shale oil have extended the lifetime of petroleum-based feedstocks,[2] biomass remains an attractive alternative because of its inherent functionality. In particular, the synthesis of highly oxygenated chemical building blocks may be more efficient starting from biomass than starting from hydrocarbons.

The combination of chemical and biological catalysis is an attractive means of producing biorenewable chemicals.[3-5] In this framework, biocatalysis is used to selectively de-functionalize biomass to yield platform species, which are then upgraded to final products using heterogeneous chemical catalysis. Thus, complex molecules that would require multiple organic syntheses or sequential biocatalytic steps can be produced using a small number of individual transformations. For example, our group has demonstrated the broad applicability of triacetic acid lactone (TAL) as a platform molecule that can be produced by polyketide biosynthesis.[6-8] In the case of 2-pyrones such as TAL, the hydrogenation of carbon-carbon double bonds is often the critical step for producing value-added chemicals. While hydrogenation catalysts are often susceptible to inhibition by biogenic impurities,[9] such deactivation can be overcome by the formation of a polymer-derived microenvironment that surrounds the active sites of the catalyst.[10]

Specialty chemicals are attractive biomass-derived products due to their high value relative to those of fuels or commodity chemicals. In addition, fine chemicals and pharmaceutical building blocks are even higher value species than specialty chemicals, making them attractive targets for biomass conversion. This work focuses on the selective hydrogenation of 4-hydroxycoumarin (4HC) as a prototypical platform chemical produced by biocatalysis that can subsequently be upgraded to fine chemicals. Notably, 4HC can be obtained in a fashion analogous to that which yields TAL, using polyketide biosynthesis in genetically engineered organisms.[11] Indeed, much of what has been learned about how to produce TAL in *E. coli* or *S. cerevisiae* can be applied to the production of 4HC because of similarities in the enzymes involved.[12]

Herein, we show that 4HC can be converted to several fine chemicals and pharmaceutical building blocks using transformations directly analogous to those involved in TAL upgrading, as outlined in Scheme 1. The partial reduction of 4HC leads to 4HDHC, which is a key intermediate for the synthesis of coumarin and dihydrocoumarin (DHC). Both coumarin and DHC are valuable as fine chemicals and chemical intermediates. In particular, coumarin is a fragrance used in soaps, lotions, and perfumes. It is also used in laser dyes, and it is a building block for several pharmaceuticals (see Boisde and Meuly[13] and the references therein). Moreover, both coumarin and DHC could be converted to the corresponding quinolones following the chemistry that has been developed for the conversion of lactones to lactams.[14] Notably, the quinolone analogue of DHC is valuable for its use as a building block for the synthesis of pharmaceutical compounds.[15, 16] Finally, we note that 4HC itself is a key intermediate in the synthesis of Warfarin,[13] an anti-clotting agent. A significant difference between 4HC upgrading and TAL upgrading pertains to the aromatic ring in 4HC. Herein, we show that the presence of this aromatic ring leads to lower catalytic activity when using monometallic Pd catalysts, likely due to high coverage of the Pd surface by 4HC bound through its aromatic ring. Furthermore, over-hydrogenation of the aromatic ring is undesirable, as this ring is required for the target products, and we show that the use of bimetallic PdAu nanoparticles leads to the high selectivities required for the production of fine chemicals and pharmaceuticals.

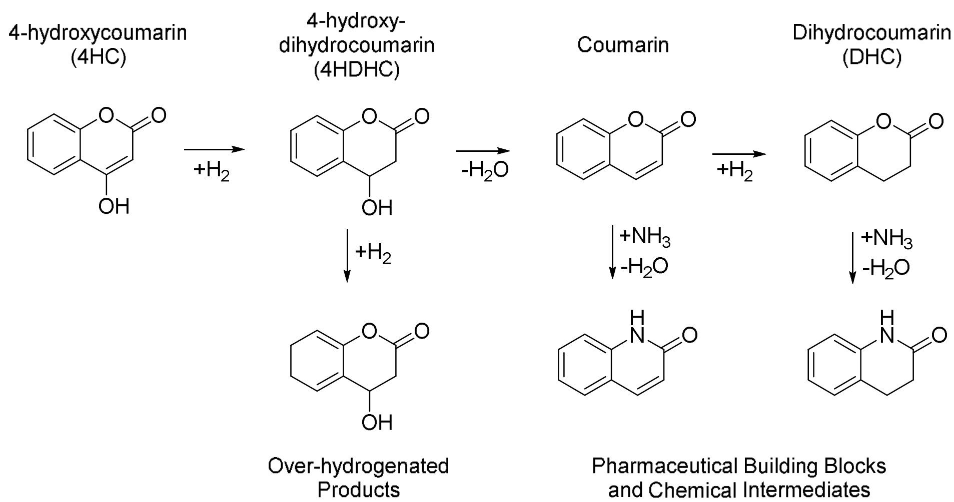


**Scheme 1.** Potential uses of 4-hydroxycoumarin (4HC), illustrating the importance of the selective hydrogenation of unsaturated carbon-carbon bonds. 4-hydroxydihydrocoumarin (4HDHC) is a key intermediate in these reactions, while coumarin and dihydrocoumarin (DHC) are valuable platform species. The conversion of lactones, such as coumarin and DHC, to their corresponding lactams has been described by Ito and Ooshida.[14]

## 2. EXPERIMENTAL DETAILS

### 2.1. CATALYST SYNTHESIS AND CHARACTERIZATION

A 10% Pd/C catalyst was purchased from Strem Chemical and used as received (Strem, Palladium, 10% on activated carbon, dry powder). The 2% Pd/$\gamma$-$Al_2O_3$, 1% Pd/Si-Al, and both the 2% and 10% low-dispersion Pd/$SiO_2$ catalysts were prepared by incipient wetness impregnation of $\gamma$-$Al_2O_3$ (Strem, low-soda), amorphous silica-alumina (Davicat 3113), or $SiO_2$ (Davisil Grade 646, crushed and sieved between 50 and 100 mesh, washed with 5% $HNO_3$ and dried in air at 383 K for 12 hr), respectively, with aqueous solutions of $Pd(NO_3)_2$ (prepared from Aldrich 10% Pd/$(NO_3)_2$ solution in 10% $HNO_3$, 99.999%). The catalysts were dried overnight in static air at 383 K, calcined at 673 K in flowing air (Airgas, medical grade USP), purged at 298 K with Ar, reduced at 773 K in flowing $H_2$ (Airgas, industrial grade), purged at 298 K with Ar, and passivated in 1% $O_2$ in Ar (Airgas, research grade). The high-dispersion 2% Pd/$SiO_2$ catalyst was prepared by ion exchange of $Pd(NO_3)_2{\cdot}4NH_3$ (Aldrich 10% $Pd(NO_3)_2{\cdot}4NH_3$ solution in water), as described previously.[9] The catalyst was dried in air at 383 K for 2 hours, calcined in air at 573 K, purged at 298 K with Ar, reduced in flowing $H_2$ at 533 K, purged at 298 K with Ar, and passivated with 1% $O_2$ in Ar. The (2%Pd-4%Au)/$Al_2O_3$ and (2%Pd-4%Au)/Si-Al catalysts were prepared by simultaneous incipient wetness impregnation of $\gamma$-$Al_2O_3$ or amorphous silica-alumina with $PdCl_2$ (Aldrich, 99.5+%) and $HAuCl_4$ (Sigma-Aldrich, 99.999%) following the method outlined by Hutchings, *et al.*, which is known to yield bimetallic nanoparticles.[17, 18] The catalysts were dried overnight in static air at 383 K, calcined at 673 K in flowing air, purged at 298 K with Ar, reduced at 773 K in flowing $H_2$, purged at 298 K with Ar, and passivated in 1% $O_2$ in Ar. The (2%Pd-4%Au)/$SiO_2$ catalyst was prepared by ion exchange, following the method of Lam and Boudart, which is known to yield bimetallic nanoparticles.[19, 20] Briefly, $[Au(en)_2]Cl_3$ was prepared from $HAuCl_4$ and ethylene diamine (Sigma-Aldrich, ≥99%) according to the procedure described by Block and Bailar.[21] The required amount of this material was dissolved in Milli-Q grade water (18 MΩ) and mixed with the required amount of $Pd(NO_3)_2 \cdot 4NH_3$ solution. This mixture was then added dropwise to a slurry of $SiO_2$ (Davisil 646, crushed and sieved between 50 and 100 mesh, washed with 5% $HNO_3$ and dried in air at 383 K for 12 hr) at 343 K. The pH of the slurry was maintained at pH 11 with $NH_4OH$ (Sigma-Aldrich, ACS Reagent 28-30% $NH_3$ basis). The suspension was stirred for 1 hour, after which it was cooled, filtered, and washed with Milli-Q grade water until the filtrate was neutral. The catalyst was dried overnight in static air at 383 K, after which it was reduced at 423 K in flowing $H_2$, purged at 298 K with Ar, and passivated in 1% $O_2$ in Ar.

The CO uptake (Airgas, 99.99%) for each reduced and passivated catalyst was measured using a Micromeritics ASAP 2020 system following reduction in flowing $H_2$ (Airgas, UHP) at 323 K. The metal dispersion of the monometallic Pd catalysts was determined based on the CO uptake with a CO:Pd stoichiometry of 0.67 unless otherwise noted. The Pd dispersion was also measured at 373 K by hydrogen (Airgas, UHP) titration of pre-adsorbed oxygen (Airgas, UHP), according to the procedure described by Benson, Hwang, and Boudart[22] and using the stoichiometry shown in Equation 1. The turnover frequencies (TOF) for the monometallic Pd catalysts were normalized to the number of Pd surface sites determined by $H_2$ titration of adsorbed O atoms. Using X-ray absorption spectroscopy (XAS) and transmission electron microscopy (TEM), it has previously been shown[20, 23] that the surfaces of bimetallic nanoparticles in high-dispersion PdAu catalysts prepared by ion exchange are highly enriched in Pd. Similar observations have been made using TEM and X-ray photoelectron spectroscopy

(XPS) for bimetallic PdAu catalysts prepared by simultaneous incipient wetness impregnation.[18] Based on XAS and TEM data, coupled with an analysis of the kinetics of cyclohexene hydrogenation, Davis and Boudart[23] suggested that TOF values for C=C bond hydrogenation using bimetallic PdAu catalysts containing small particles are most appropriately normalized to the total Pd loading. We have used this approach to calculate our TOF values.

$$Pd_S O + \tfrac{3}{2} H_2 \rightarrow Pd_S H + H_2O \qquad \text{Equation 1}$$

## 2.2. REACTION KINETICS MEASUREMENTS

Hydrogenation of 4HC was carried out in a 50 mL Hastelloy pressure vessel (Parr Instrument, model 4792). The catalyst and magnetic stir bar were loaded into the reactor with a feed solution containing 4HC (Aldrich, 98%) or coumarin (Aldrich, ≥98%) dissolved in tetrahydrofuran (Fisher, Certified Grade). The vessel was then sealed, purged with Ar, and pressurized with 27 bar of $H_2$. Unless otherwise noted, reaction kinetics measurements were carried out at 348 K (5 K $min^{-1}$) with 27 bar of $H_2$, and the vessel was stirred at 500 rpm. For measurement of the reaction orders and activation barriers, samples were periodically withdrawn from the reactor through a dip tube, and the initial TOF and corresponding 95% confidence interval were determined based on the slope of the plot of concentration versus time. A sample was withdrawn after the reactor reached the selected reaction temperature, and this point was chosen as zero-time. Negligible conversion was observed during the heat-up period. The absence of mass transfer limitations was verified by evaluating the Weisz-Prater number (see Section 1 of the Supporting Information).

Due to its thermal instability, the concentration of 4HC was determined by high performance liquid chromatography (HPLC) (Waters Alliance 2695 equipped with a Waters 996 UV detector and a reversed-phase Agilent Zorbax SB-C18 column (4.6 x 300 mm, 5 μm) using 5 mM $H_2SO_4$

as the aqueous phase with acetonitrile as the organic modifier). The concentrations of 4HDHC, coumarin, DHC, and the over-hydrogenated product were determined by gas chromatography (GC) (Shimadzu GC2010 equipped with an FID and a DB-5MS capillary column). The identities of the species were verified using gas chromatography/mass spectrometry (GC/MS) (Shimadzu GCMS-QP2010S equipped with a SHRXI-5MS capillary column), and the spectra were compared with those in the NIST MS spectral library.

## 2.3 IN SITU INFRARED SPECTROSCOPY

A specially configured Hastelloy autoclave (Parr Instrument, modified from model 4590) was used to collect *in situ* attenuated total reflectance Fourier transform infrared (ATR-FTIR) spectra. The spectra were obtained using a Mettler-Toledo AutoChem ReactIR iC10 spectrometer equipped with a photoconductive detector (MCT type). The spectrometer interfaces with the reactor using a 9.5 mm AgX DiComp Diamond ATR probe that enters the reactor at an angle from the bottom. A background spectrum was first obtained of the probe sealed in an empty reactor at ambient temperature. Then, the catalyst and a feed solution consisting of 4HC dissolved in THF were charged to the reactor, which was sealed, purged with He, and pressurized with $H_2$. The reactor was then heated to 348 K (1.67 K $min^{-1}$), and stirring was maintained at 500 rpm using an overhead mechanical stirrer. An absorbance spectrum was collected every 15 minutes consisting of 256 co-averaged scans taken at 4 $cm^{-1}$ resolution and referenced to the background spectrum of the empty reactor at ambient temperature. Baseline drift with respect to reaction time was accounted for by measuring the peak height with respect to the flat baseline adjacent to the peak. In some experiments, samples were periodically withdrawn through a dip tube and the concentrations of the species in solution were measured by HPLC and GC as described above.

Spectral assignments were made based on spectra predicted by density functional theory (DFT). Calculations were performed using Gaussian09 software.[24] Geometry optimizations and frequency calculations were performed at the B3LYP/6-31+G(d,p) level of theory. Solvation effects were accounted for by the SMD solvation model using a THF dielectric medium. The vibrational frequencies of the bonds of interest were scaled based on the difference between the predicted and experimental frequency of the C-O bond in THF.

## 3. RESULTS AND DISCUSSION

Several fine chemicals can be obtained from 4HC using a set of reactions analogous to those required for TAL upgrading.[8] The unsaturated carbon-carbon bond in the lactone ring of 4HC can be hydrogenated using supported Pd catalysts (Entries 1-4, Table 1), consistent with previous reports.[25-28] Notably, some DHC is observed in these reactions. It is known that acid sites[29, 30] or oxophilic sites[31] are needed for C-O hydrogenolysis to occur over Pd-based catalysts at the mild conditions used here, which suggests that the formation of DHC may be due to 4HDHC dehydration by acidic impurities on the catalyst support, yielding coumarin, which is easily hydrogenated to dihydrocoumarin (DHC) at these reaction conditions (Entries 8 and 9, Table 1). The silica gel support appears to have the least amount of acidic impurities, and by using a 2% Pd/$SiO_2$ catalyst we obtained 93% selectivity to hydrogenated products (4HDHC and DHC) at 82% 4HC conversion. In all three cases, we observed a small amount of selectivity to an over-hydrogenated form of 4HDHC, where the aromatic ring was partially saturated.

A catalyst containing both metal and acid sites could lead to the direct production of DHC from 4HC. Importantly, this reaction can proceed with high selectivity because 4HC cannot undergo the same retro Diels-Alder reaction that prevents the direct conversion of TAL to δ-hexalactone.[32] Accordingly, we synthesized a Pd catalyst supported on amorphous silica-alumina. At the same reaction conditions used for the hydrogenation of 4HC to 4HDHC, this catalyst led to 71% DHC selectivity at 87% 4HC conversion (Entry 4, Table 1). Notably, the only other products formed were 4HDHC (22% selectivity) and the over-hydrogenated form of 4HDHC (7% selectivity). Based on these results and our previously described acid-catalyzed dehydration of hydroxy-pyrones,[8] we suggest that coumarin could also be produced from 4HC by the dehydration of 4HDHC.

**Table 1.** Hydrogenation of 4-hydroxycoumarin using Pd-based catalysts[a]

| **Entry** | **Catalyst** | **Reactant** | **Cat:Feed (g:g)** | **Time (h)** | **Conv (%)** | **Sel to 4HDHC (%)** | **Sel to DHC (%)** | **Sel to Overhyd. (%)** | **Init. TOF. ($ks^{-1}$)[b]** |
|---|---|---|---|---|---|---|---|---|---|
| **1** | 10% Pd/C | 4HC | 0.17 | 5 | 78 | 79 | 14 | 5 | 8.5 |
| **2** | 2%Pd/$Al_2O_3$ | 4HC | 0.69 | 12 | 88 | 78 | 16 | 6 | 2.9 |
| **3** | 2%Pd/$SiO_2$ | 4HC | 0.33 | 27 | 82 | 85 | 8 | 7 | 2.2 |
| **4** | 1%Pd/Si-Al | 4HC | 0.34 | 48 | 87 | 22 | 71 | 7 | -- |
| **5** | PdAu/$Al_2O_3$[c] | 4HC | 0.17 | 19 | 87 | 83 | 17 | <1 | 6.1 |
| **6** | PdAu/$SiO_2$[c] | 4HC | 0.17 | 12 | 86 | 87 | 10 | 3 | 5.0 |
| **7** | PdAu/Si-Al[c] | 4HC | 0.88 | 48 | 90 | 12 | 86 | 2 | -- |
| **8** | 2%Pd/$Al_2O_3$ | Coumarin | 0.17 | 2 | >99 | -- | >99 | n.d.[d] | -- |
| **9** | PdAu/$SiO_2$[c] | Coumarin | 0.17 | 2 | >99 | -- | >99 | n.d.[d] | -- |

a) Reaction conditions: 2 wt% reactant in tetrahydrofuran, 348 K, 27 bar $H_2$. b) Initial TOF measured at conversions below 15%. Calculated based on surface Pd measured by $H_2$ titration of adsorbed O atoms (monometallic Pd catalysts) or total Pd (bimetallic Pd catalysts) according to Davis and Boudart.[23] c) PdAu catalysts are 2 wt% Pd and 4 wt% Au. d) Not detected.

The use of monometallic Pd catalysts leads to high but not quantitative selectivity for hydrogenation of the carbon-carbon double bond in the lactone ring of 4HC. In each case (see Entries 1-4 in Table 1), some of the 4HDHC is over-hydrogenated (*i.e.*, the aromatic ring is partially saturated), achieving 6-7% selectivity to the over-hydrogenated species at 78-88% 4HC conversion. We used a batch reactor equipped with an *in situ* ATR-FTIR probe to monitor the time-evolution of these consecutive reactions. Figure 1a shows the time-evolution of the FTIR spectra between 1600-1800 $cm^{-1}$. Three IR bands are highlighted that correspond to the C=C stretch in 4HC (1630 $cm^{-1}$), the C=O stretch in both 4HDHC and DHC (overlapping absorbances at 1780 $cm^{-1}$), and the asymmetric diene stretch in the over-hydrogenated product (1744 $cm^{-1}$, see Scheme 1). Figures S1-S4 show the infrared spectra predicted for these molecules using density functional theory. Note that the band at 1744 $cm^{-1}$ overlaps with the C=O stretch in 4HC (1735 $cm^{-1}$), so the absorbance at short reaction times is dominated by contributions from 4HC. Figure 1b shows that the absorbance at 1780 $cm^{-1}$ exhibits the behavior of an intermediate species and passes through a maximum in intensity with respect to reaction time. The appearance of this band corresponds to the disappearance of the band at 1630 $cm^{-1}$. The decrease in the intensity of the band at 1780 $cm^{-1}$ corresponds to an increase in the intensity of the band at 1744 $cm^{-1}$.

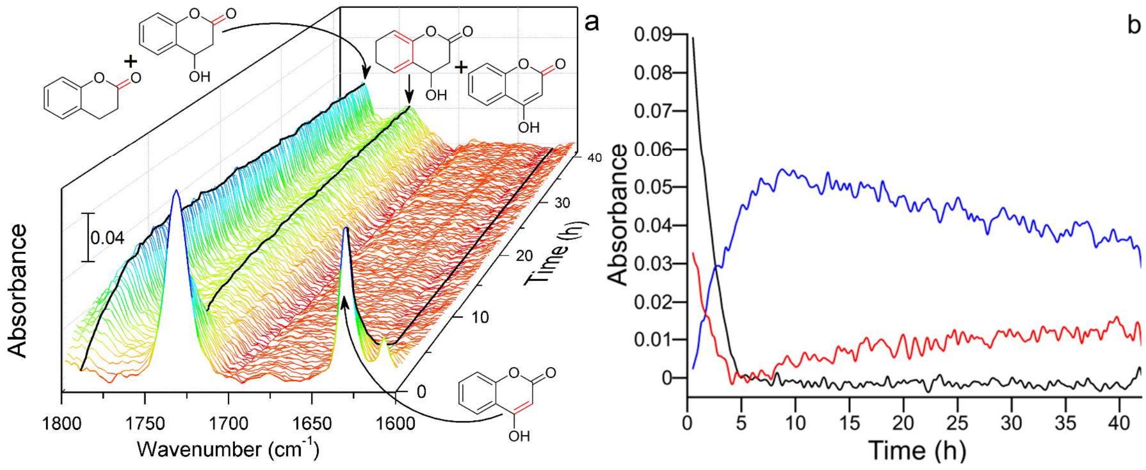


**Figure 1.** Hydrogenation of 4HC using 10%Pd/C, monitored by *in situ* ATR-FTIR spectroscopy. (a) Changes in IR spectra with respect to reaction time, with the three absorbances of interest highlighted. (b) Changes in IR absorbance with respect to reaction time. The absorbance at 1630 $cm^{-1}$ corresponds to 4HC (black), the absorbance at 1780 $cm^{-1}$ corresponds to 4HDHC and DHC (blue), and the absorbance at 1744 $cm^{-1}$ corresponds to the over-hydrogenated product (red). Reaction conditions: 348 K, 27 bar $H_2$, 133 mM 4HC in THF, cat:4HC = 0.42 g:g, $Pd_s$:4HC = 0.01 mol:mol.

Figure 2a shows that a similar trend is obtained for the 2% $Pd/SiO_2$ catalyst, although as shown in Table 1, the TOF is much lower for the silica-supported catalyst than for the carbon-supported catalyst. The reactor was sampled periodically during this reaction, and the concentrations of species in solution were measured by HPLC and GC. As shown in Figures 3a-c, the reaction profiles generated by HPLC and GC are consistent with those generated by *in situ* ATR-FTIR spectroscopy.

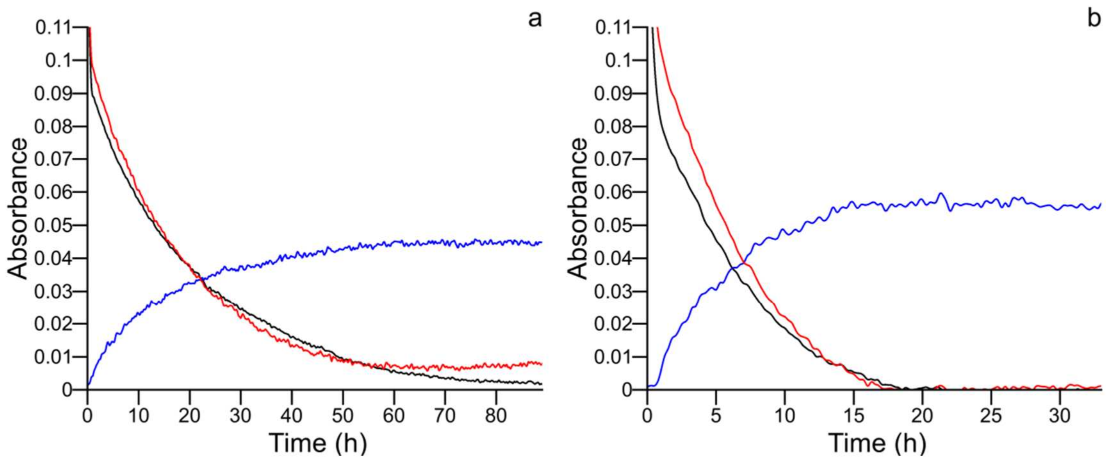


**Figure 2.** Infrared absorbance versus reaction time for the hydrogenation of 4HC using 2% Pd/$SiO_2$ (a) and (2% Pd-4% Au)/$SiO_2$ (b). The absorbance at 1630 $cm^{-1}$ corresponds to 4HC (black), the absorbance at 1780 $cm^{-1}$ corresponds to 4HDHC and DHC (blue), and the absorbance at 1744 $cm^{-1}$ corresponds to the overhydrogenated product (red). Reaction conditions: 348 K, 27 bar $H_2$, 133 mM 4HC in THF, cat:4HC = 0.42 g:g, (a) $Pd_s$:4HC = 0.009 mol:mol, (b) $Pd_s$:4HC = 0.13 mol:mol.

Achieving high selectivity is important for the stringent purity specifications demanded by the fine chemicals and pharmaceuticals markets.[33] Consequently, the key bottleneck for upgrading 4HC will be the selective hydrogenation of the unsaturated carbon-carbon bond without over-hydrogenating the aromatic ring (to produce either 4HDHC or DHC). We have observed that the formation of bimetallic PdAu nanoparticles decreases the over-hydrogenation activity of the monometallic Pd materials, with the combined selectivity to 4HDHC and DHC increasing from 93% for the 2% Pd/$SiO_2$ catalyst to 97% for the (2% Pd-4% Au)/$SiO_2$ catalyst, as an example (Entries 3 and 6, Table 1). As shown in Figure 2b, no over-hydrogenated products were detected when using this catalyst for 15 hours beyond the time required for complete conversion of 4HC, nor were any over-hydrogenated products detected when using the (2% Pd-4% Au)/$Al_2O_3$

catalyst (see Entry 5, Table 1). Also notable is the increase in the TOF that accompanies the addition of Au, with the initial TOF for the (2% Pd-4% Au)/$SiO_2$ catalyst more than double that of the 2% Pd/$SiO_2$ catalyst. Similar improvements were also observed when using $\gamma$-$Al_2O_3$ and amorphous $SiO_2$-$Al_2O_3$ as supports (see Table 1).

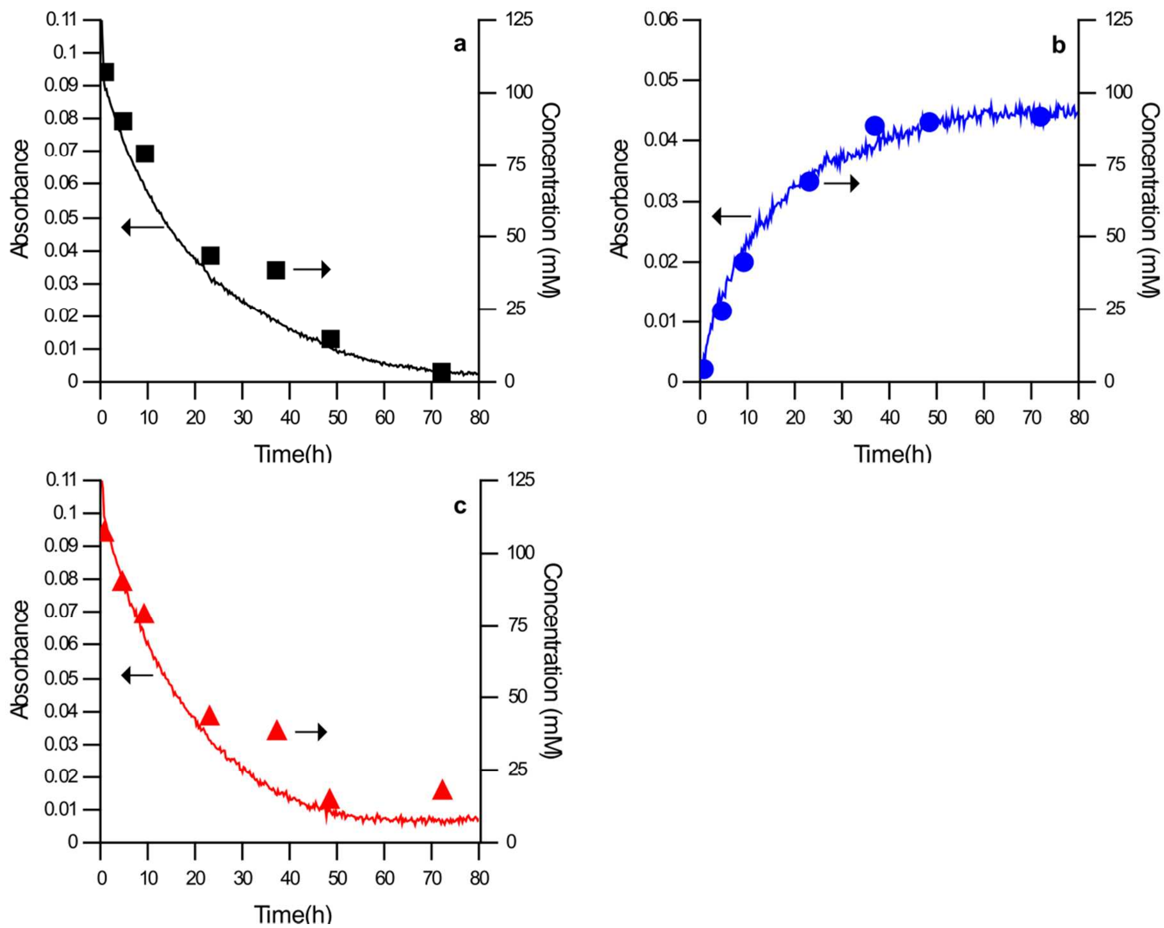


**Figure 3.** Infrared absorbance versus reaction time for the hydrogenation of 4HC using 2% Pd/$SiO_2$. Comparison of HPLC and GC data (points) with FTIR absorbance data (lines) for: (a) the band at 1630 $cm^{-1}$ (4HC), (b) the band at 1780 $cm^{-1}$ (4HDHC and DHC), and (c) the band at 1744 $cm^{-1}$ (the over-hydrogenated product and 4HC). Reaction conditions: 348 K, 27 bar $H_2$, 133 mM 4HC in THF, cat:4HC = 0.42 g:g, $Pd_s$:4HC = 0.009 mol:mol.

The TOF for 4HDHC formation is significantly higher when using the 10% Pd/C catalyst than when using the 2% Pd/$SiO_2$ catalyst (comparing Entries 1 and 3 in Table 1). As shown in Table 2, which lists the Pd dispersion, $D$, and the nanoparticle size (calculated as 1.1/$D$) for the catalysts used in this study, the 10% Pd/C catalyst has a substantially lower Pd dispersion than does the 2% Pd/$SiO_2$ catalyst. To rule out the possibility of an influence of the support on the rate of 4HDHC production, we prepared a 2% Pd/$SiO_2$ catalyst with a 6% Pd dispersion. As shown in Figure 4, the initial TOF obtained using this catalyst was higher than that for the 10% Pd/C catalyst, which has a 16% Pd dispersion. Indeed, Figure 4 shows that the TOF for the formation of 4HDHC is dependent on the metal nanoparticle size, and is independent of the nature of the support.

**Table 2.** Metal dispersion of the monometallic catalysts used in this study[a]

| **Entry** | **Catalyst** | **Nominal metal loading (μmol/g)** | **$H_2$ Uptake (μmol/g)** | **Pd Dispersion (*D*) (%)[b]** | **Pd nanoparticle size (nm)[c]** |
|---|---|---|---|---|---|
| **1** | 10% Pd/C | 940 | 218 | 16 | 7.1 |
| **2** | 2% Pd/$Al_2O_3$ | 188 | 125 | 44 | 2.5 |
| **3** | 2% Pd/$SiO_2$ | 188 | 195 | 70 | 1.6 |
| **4** | 1% Pd/Si-Al | 94 | 65 | 46 | 2.4 |
| **5** | 2% Pd/$SiO_2$ | 188 | 18 | 6 | 17 |

a) The Pd dispersion measured by CO chemisorption can be found in Table S1. b) Assuming $Pd_SO + \frac{3}{2}H_2 \rightarrow Pd_SH + H_2O$. Figure S5 shows the hydrogen titration data for Entry 3. c) Calculated as 1.1/$D$, using the $H_2$ titration data and assuming spherical particles.

In conjunction with the decrease in the 4HDHC formation rate when using small Pd nanoparticles, the rate of over-hydrogenation by the high-dispersion 2% Pd/$SiO_2$ catalyst is qualitatively lower than that by the low-dispersion 10% Pd/C catalyst (comparing Figure 1b with Figure 2a). Interestingly, Somorjai and coworkers observed a similar effect for the hydrogenation of benzene and toluene using SBA-15-supported Pt catalysts.[34] These authors note that the activation barrier for the hydrogenation of both benzene and toluene decreases with increasing Pt particle size, consistent with the qualitative increase in over-hydrogenation rate observed in our work.

We have observed that the hydrogenation of 4HC by the high-dispersion 2% Pd/$SiO_2$ catalyst is negative-order with respect to 4HC, indicating that the Pd surface is highly covered by 4HC (see Figure S7). However, the reaction is nearly zero-order with respect to 4HC when catalyzed by a 10% Pd/$SiO_2$ catalyst that has a low metal dispersion, indicating that the surface coverage by 4HC decreases with increasing particle size. The reaction order with respect to hydrogen is unaffected by particle size, as is the apparent activation barrier (see Figures S8 and S9), indicating the mechanism is the same over both catalysts and the observed changes in rate are due to surface coverage effects. Because the rate of over-hydrogenation is slow over both catalysts, we postulate that aromatically-bound 4HC acts as a spectator species occupying sites that would otherwise be active for 4HC hydrogenation. Stronger bonding of these aromatic species on the low-coordination sites of the more highly dispersed Pd nanoparticles would lead to more extensive blocking of the active sites and thus lower catalytic activity.

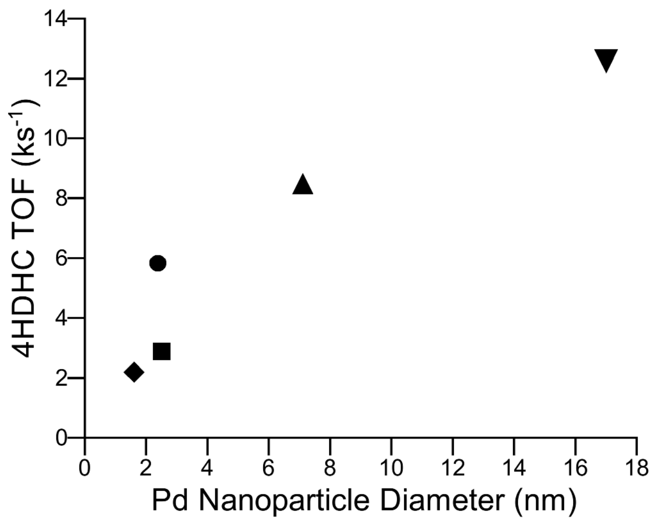


**Figure 4.** Influence of Pd nanoparticle size on the TOF for 4HDHC formation. 2% Pd/$SiO_2$ (♦), 2% Pd/$Al_2O_3$ (■), 1% Pd/Si-Al (●), 10% Pd/C (▲), and 2% Pd/$SiO_2$ (▼). The nanoparticle size, *d*, was determined assuming spherical particles and based on the metal dispersion, *D*, as $d$=1.1/$D$.

A significant improvement in selectivity is achieved when using the PdAu catalysts. Puddu and Ponec observed a similar effect for benzene hydrogenation by PtAu alloys, whereby the addition of small amounts of Au to Pt completely deactivated the catalyst towards benzene hydrogenation.[35] It is difficult to determine whether this observation was due to an electronic effect that would lead to a high barrier for aromatic hydrogenation or due to a geometric effect. Notably, in the case of 4HC hydrogenation, the reaction is negative-order with respect to the hydrocarbon when using both highly-dispersed Pd and PdAu catalysts, suggesting that the surface coverage by 4HC is not affected by alloying.

Davis and Boudart[23] found that the rate of cyclohexene hydrogenation over a $SiO_2$-supported PdAu catalyst is best described by a TOF normalized to the total amount of Pd rather than one normalized to surface Pd sites counted by chemisorption. This observation indicates that, in the presence of hydrocarbons, the surface of the PdAu nanoparticles is highly-enriched by Pd, in-line with observations that the surface of PdAu bimetallic nanoparticles can restructure in response to adsorption of species that bind strongly to Pd.[36, 37] Importantly, the rate of 4HC hydrogenation increases by a factor of two upon formation of bimetallic PdAu nanoparticles, consistent with the observations of Davis and Boudart. Consequently, we postulate that, under the conditions of 4HC hydrogenation, the surface of the PdAu nanoparticles is enriched by Pd, which is highly covered by 4HC bound through its aromatic ring. The presence of subsurface Au modifies the catalyst to prevent saturation of the aromatic ring, as described by Puddu and Ponec for PtAu, such that the aromatically-bound 4HC remains on the surface as a spectator species, as described for the monometallic Pd catalysts. Consequently, the remaining vacant sites are more active for hydrogenation of the unsaturated carbon-carbon bond in the lactone ring of 4HC, consistent with the observations of Davis and Boudart.

## 4. CONCLUSIONS

In this work we found that the selective reduction of unsaturated carbon-carbon bonds can proceed in the presence of aromatic rings, enabling the production of high-value products from biomass using biologically-derived platform intermediates. In particular, 4HC can be upgraded to several fine chemicals and pharmaceutical building blocks, all of which require the selective hydrogenation of 4HC to 4HDHC. This reaction proceeds over Pd-based catalysts, and the highest selectivities were obtained using bimetallic PdAu catalysts. Both the surface coverage by 4HC and its rate of hydrogenation are dependent on metal nanoparticle size for monometallic Pd catalysts, likely due to changes in the activation barrier for saturation of the aromatic ring in 4HC. The addition of Au to the catalyst led to a factor-of-two increase in the TOF for 4HDHC production.

ASSOCIATED CONTENT

**Supporting Information**. Evaluations of potential mass transport limitations, predicted FTIR spectra for the reactants and products, representative plots of CO and $H_2$ uptake for the monometallic Pd catalysts, dispersion measurements by CO chemisorption, and measurements of the apparent reaction kinetics using the low- and high-dispersion $Pd/SiO_2$ catalysts and the $PdAu/SiO_2$ catalyst. This material is available free of charge via the Internet at http://pubs.acs.org.

AUTHOR INFORMATION

**Corresponding Author**

*E-mail: jdumesic@wisc.edu

**Present Addresses**

† Department of Chemical and Biological Engineering, University of Maine, Orono, ME 04469

ACKNOWLEDGMENT

This material is based upon work supported by the National Science Foundation Engineering Research Center for Biorenewable Chemicals (CBiRC) under Award No. EEC-0813570. Portions of the ATR-FTIR apparatus were purchased with support in part from the Advanced Biofuel Intermediates program of the U.S. Forest Service and in part by the Agriculture and Food Research Initative Grant No. 2011-67009-20056 from the USDA National Institute of Food and Agriculture. T.J.S. acknowledges support from the National Science Foundation Graduate Research Fellowship Program under Grant No. DGE-1256259. Any opinions, findings, and conclusions or recommendations expressed in this material are those of the authors and do not necessarily reflect the views of the National Science Foundation.

REFERENCES

1. Bozell, J. J., *Clean: Soil, Air, Water* **2008**, 36, 641-647.
2. U.S. Crude Oil Production to 2025: Updated Projection of Crude Types. U.S. Energy Information Administration: 2015.
3. Schwartz, T. J.; O'Neill, B. J.; Shanks, B. H.; Dumesic, J. A., *ACS Catal.* **2014**, 4, 2060-2069.
4. Nikolau, B. J.; Perera, M.; Brachova, L.; Shanks, B., *Plant J.* **2008**, 54, 536-545.
5. Shanks, B. H., *ACS Chem. Biol.* **2007**, 2, 533-535.
6. Cardenas, J.; Da Silva, N. A., *Metab. Eng.* **2014**, 25, 194-203.
7. Xie, D. M.; Shao, Z. Y.; Achkar, J. H.; Zha, W. J.; Frost, J. W.; Zhao, H. M., *Biotechnol. Bioeng.* **2006**, 93, 727-736.
8. Chia, M.; Schwartz, T. J.; Shanks, B. H.; Dumesic, J. A., *Green Chem.* **2012**, 14, 1850-1854.
9. Schwartz, T. J.; Brentzel, Z. J.; Dumesic, J. A., *Catal. Lett.* **2015**, 145, 15-22.
10. Schwartz, T. J.; Johnson, R. L.; Cardenas, J.; Okerlund, A.; Da Silva, N. A.; Schmidt-Rohr, K.; Dumesic, J. A., *Angew. Chem. Int. Ed.* **2014**, 53, 12718-12722.
11. Liu, B.; Raeth, T.; Beuerle, T.; Beerhues, L., *Plant Mol. Biol.* **2010**, 72, 17-25.
12. Stewart Jr, C.; Vickery, C. R.; Burkart, M. D.; Noel, J. P., *Curr. Opin. Plant Biol.* **2013**, 16, 365-372.
13. Boisde, P. M.; Meuly, W. C., Coumarin. In *Kirk-Othmer Encyclopedia of Chemical Technology*, John WIley & Sons: 2014; pp 1-10.
14. Ito, M.; Ooshida, T. Production of Epsilon-Caprolactam. JP4164603, 1997.
15. Sridharan, V.; Suryavanshi, P. A.; Menendez, J. C., *Chem. Rev.* **2011**, 111, 7157-7259.
16. Felpin, F.-X.; Coste, J.; Zakri, C.; Fouquet, E., *Chem. - Eur. J.* **2009**, 15, 7238-7245.
17. Edwards, J. K.; Solsona, B.; Ntainjua, N. E.; Carley, A. F.; Herzing, A. A.; Kiely, C. J.; Hutchings, G. J., *Science* **2009**, 323, 1037-1041.
18. Edwards, J. K.; Solsona, B. E.; Landon, P.; Carley, A. F.; Herzing, A.; Kiely, C. J.; Hutchings, G. J., *J. Catal.* **2005**, 236, 69-79.
19. Lam, Y. L.; Boudart, M., *J. Catal.* **1977**, 50, 530-540.
20. Davis, R. J.; Boudart, M., *J. Phys. Chem.* **1994**, 98, 5471-5477.
21. Block, B. P.; Bailar, J. C., *J. Am. Chem. Soc.* **1951**, 73, 4722-4725.
22. Benson, J. E.; Hwang, H. S.; Boudart, M., *J. Catal.* **1973**, 30, 146-153.
23. Davis, R. J.; Boudart, M. *Hydrogenation of alkenes on supported palladium-gold clusters*, Catalytic Science and Technology: Proceedings of the First Tokyo Conference on Advanced Catalytic Science and Technology, Tokoyo, Kodansha: Tokoyo, 1991; pp 129-134.
24. Frisch, M. J.; Trucks, G. W.; Schlegel, H. B.; Scuseria, G. E.; Robb, M. A.; Cheeseman, J. R.; Scalmani, G.; Barone, V.; Mennucci, B.; Petersson, G. A.; Nakatsuji, H.; Caricato, M.; Li, X.; Hratchian, H. P.; Izmaylov, A. F.; Bloino, J.; Zheng, G.; Sonnenberg, J. L.; Hada, M.; Ehara, M.; Toyota, K.; Fukuda, R.; Hasegawa, J.; Ishida, M.; Nakajima, T.; Honda, Y.; Kitao, O.; Nakai, H.; Vreven, T.; Montgomery, J. J. A.; Peralta, J. E.; Ogliaro, F.; Bearpark, M.; Heyd, J. J.;

Brothers, E.; Kudin, K. N.; Staroverov, V. N.; Kobayashi, R.; Normand, J.; Raghavachari, K.; Rendell, A.; Burant, J. C.; Iyengar, S. S.; Tomasi, J.; Cossi, M.; Rega, N.; Millam, N. J.; Klene, M.; Knox, J. E.; Cross, J. B.; Bakken, V.; Adamo, C.; Jaramillo, J.; Gomperts, R.; Stratmann, R. E.; Yazyev, O.; Austin, A. J.; Cammi, R.; Pomelli, C.; Ochterski, J. W.; Martin, R. L.; Morokuma, K.; Zakrzewski, V. G.; Voth, G. A.; Salvador, P.; Dannenberg, J. J.; Dapprich, S.; Daniels, A. D.; Farkas, Ö.; Foresman, J. B.; Ortiz, J. V.; Cioslowski, J.; Fox, D. J. *Gaussian 09, Revision C.01*, Gaussian, Inc.: Wallingford, CT, 2009.

25. Huck, W. R.; Bürgi, T.; Mallat, T.; Baiker, A., *J. Catal.* **2003**, 219, 41-51.

26. Huck, W. R.; Bürgi, T.; Mallat, T.; Baiker, A., *J. Catal.* **2001**, 200, 171-180.

27. Huck, W.-R.; Mallat, T.; Baiker, A., *J. Catal.* **2000**, 193, 1-4.

28. Huck, W.-R.; Mallat, T.; Baiker, A., *New J. Chem.* **2002**, 26, 6-8.

29. Zhao, C.; He, J.; Lemonidou, A. A.; Li, X.; Lercher, J. A., *J. Catal.* **2011**, 280, 8-16.

30. Marin-Flores, O. G.; Karim, A. M.; Wang, Y., *Catal. Today* **2014**, 237, 118-124.

31. de Souza, P.; Nie, L.; Borges, L. P.; Noronha, F.; Resasco, D., *Catal. Lett.* **2014**, 144, 2005-2011.

32. Chia, M.; Haider, M. A.; Pollock, G., III; Kraus, G. A.; Neurock, M.; Dumesic, J. A., *J. Am. Chem. Soc.* **2013**, 135, 5699-5708.

33. Pollak, P., *Fine Chemicals : The Industry and the Business (2nd Edition)*. John Wiley & Sons: Hoboken, NJ, USA, 2011.

34. Pushkarev, V. V.; An, K.; Alayoglu, S.; Beaumont, S. K.; Somorjai, G. A., *J. Catal.* **2012**, 292, 64-72.

35. Puddu, S.; Ponec, V., *Recl. Trav. Chim. Pays-Bas* **1976**, 95, 255-284.

36. Kunz, S.; Iglesia, E., *J. Phys. Chem. C* **2014**, 118, 7468-7479.

37. Gao, F.; Wang, Y.; Goodman, D. W., *J. Phys. Chem. C* **2009**, 113, 14993-15000.

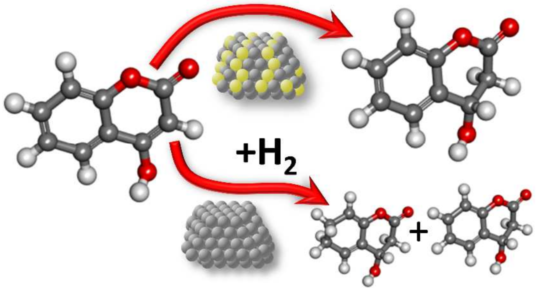


The use of supported bimetallic PdAu catalysts allows for the highly selective hydrogenation of unsaturated carbon-carbon bonds in the presence of aromatic rings.

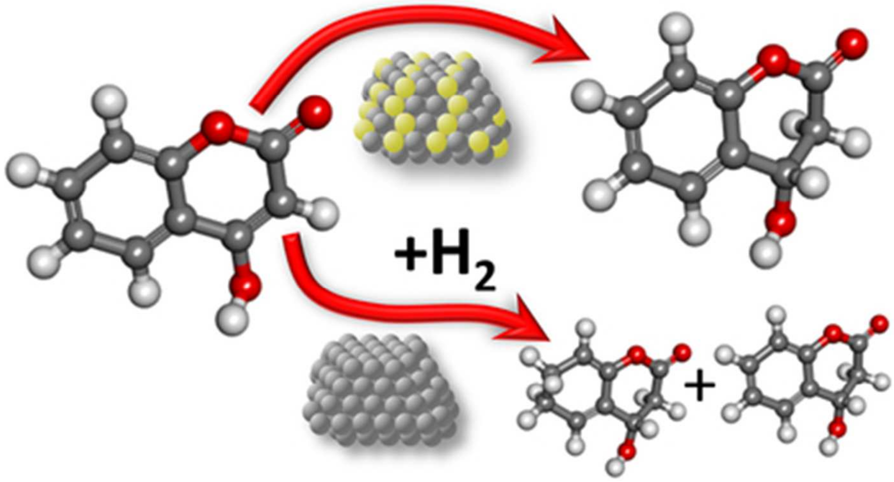


Graphical abstract
38x20mm (300 x 300 DPI)

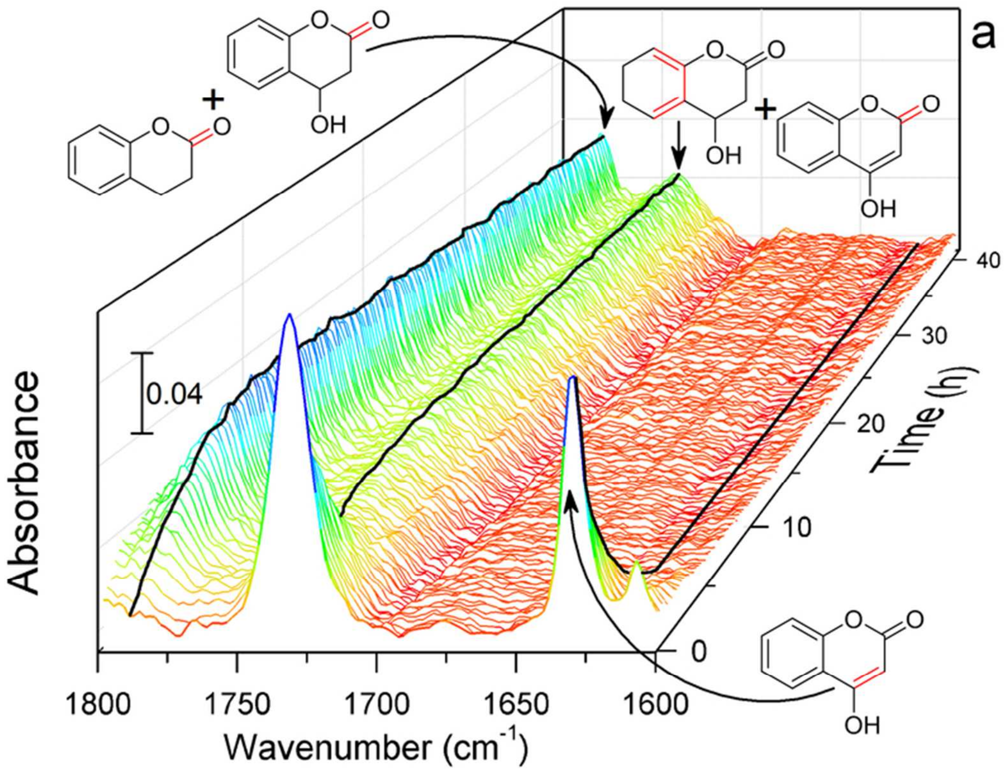


Figure 1a
66x51mm (300 x 300 DPI)

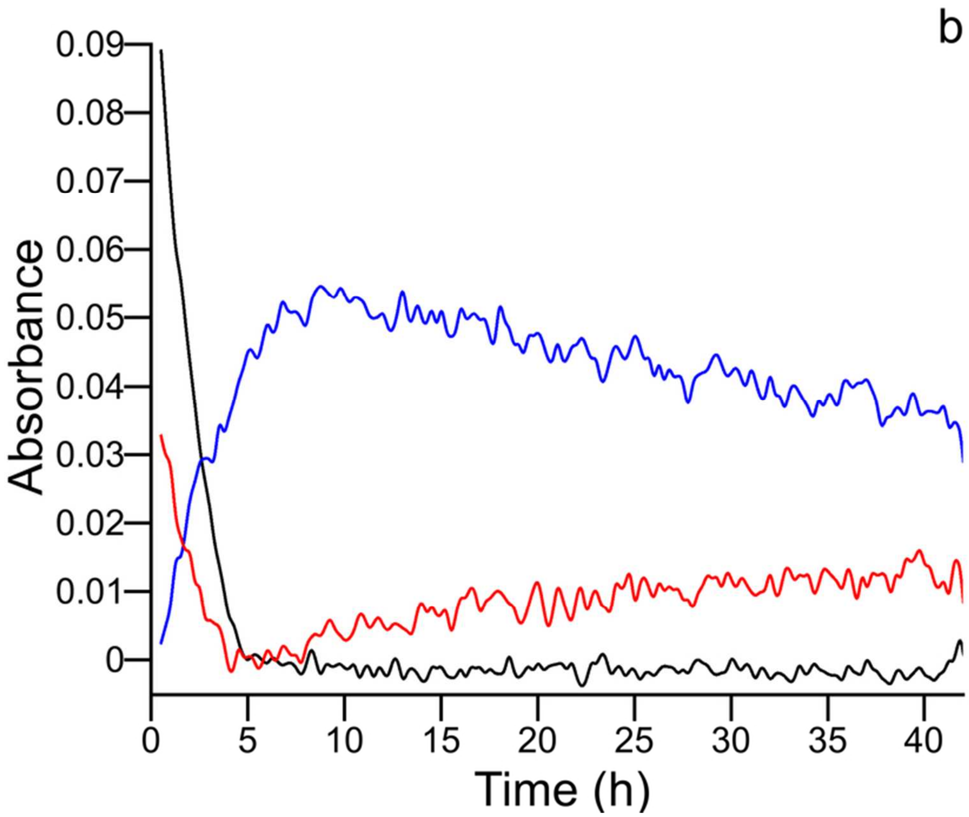


Figure 1b
71x59mm (300 x 300 DPI)

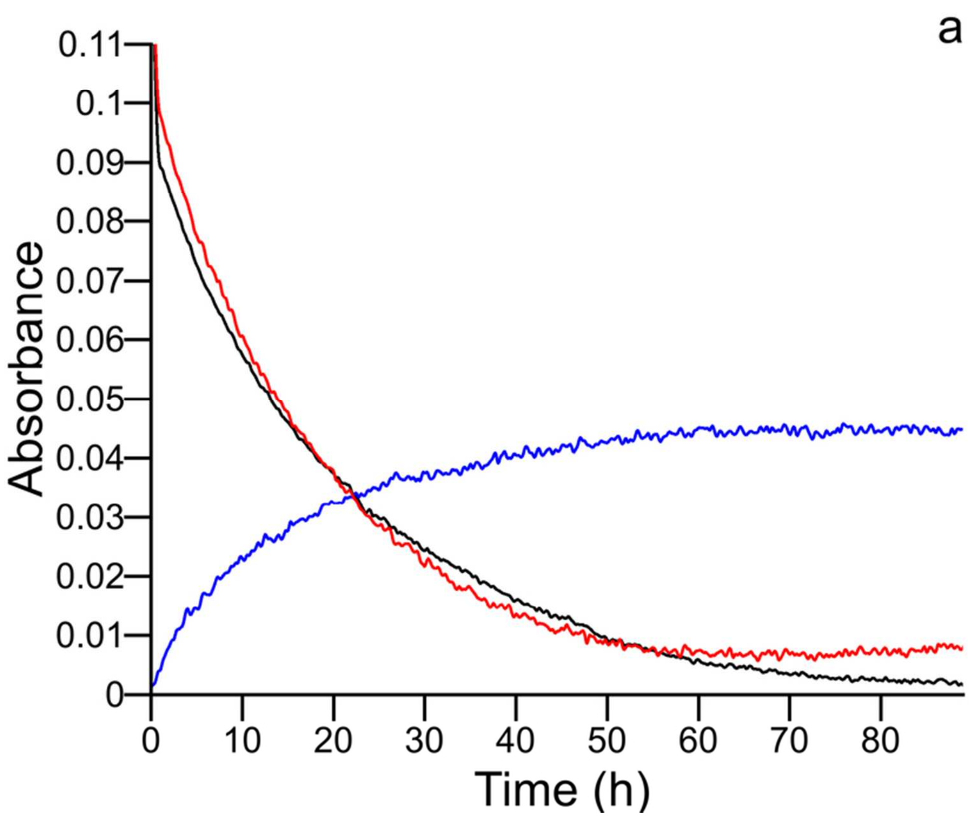


Figure 2a
71x59mm (300 x 300 DPI)

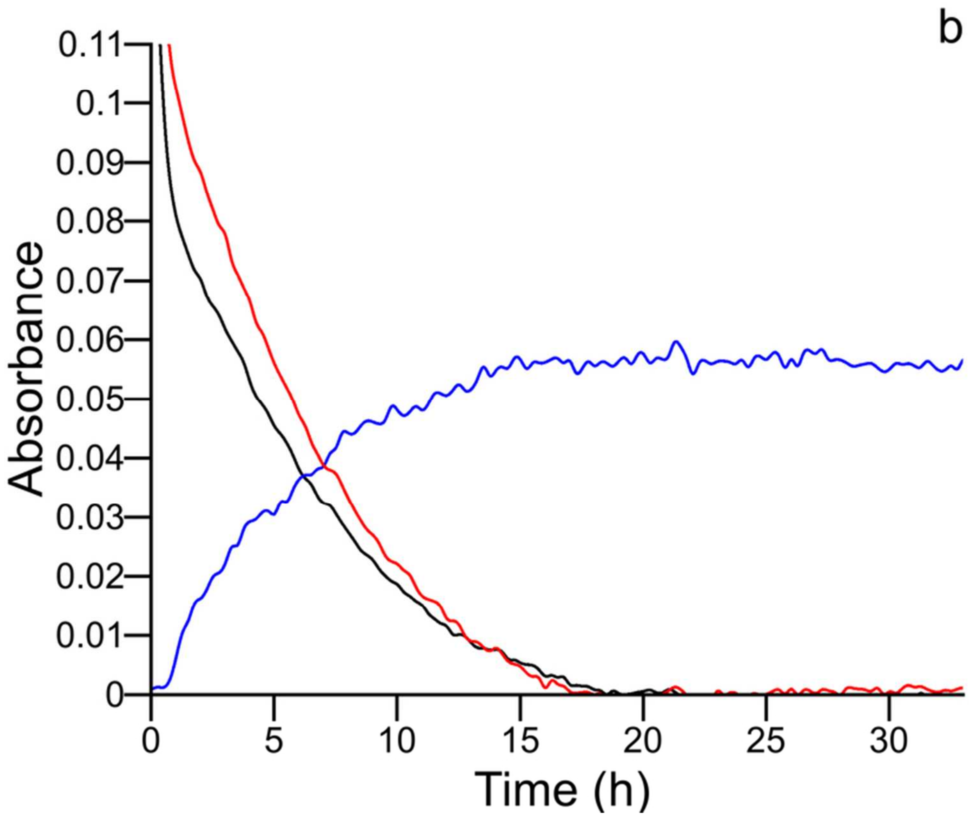


Figure 2b
71x59mm (300 x 300 DPI)

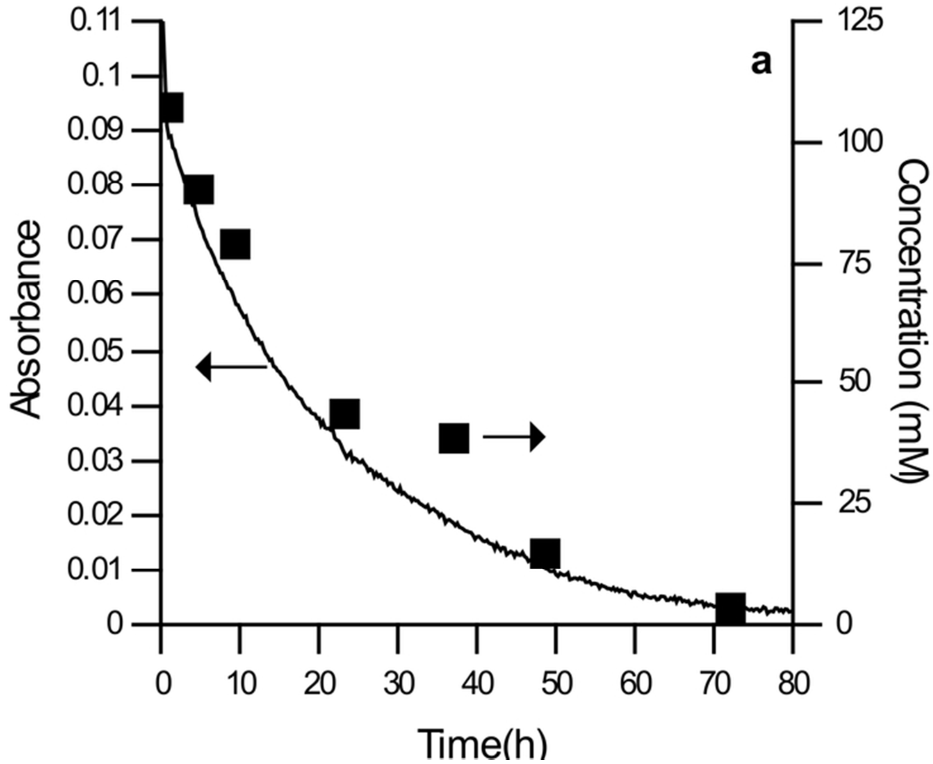


Figure 3a
66x51mm (300 x 300 DPI)

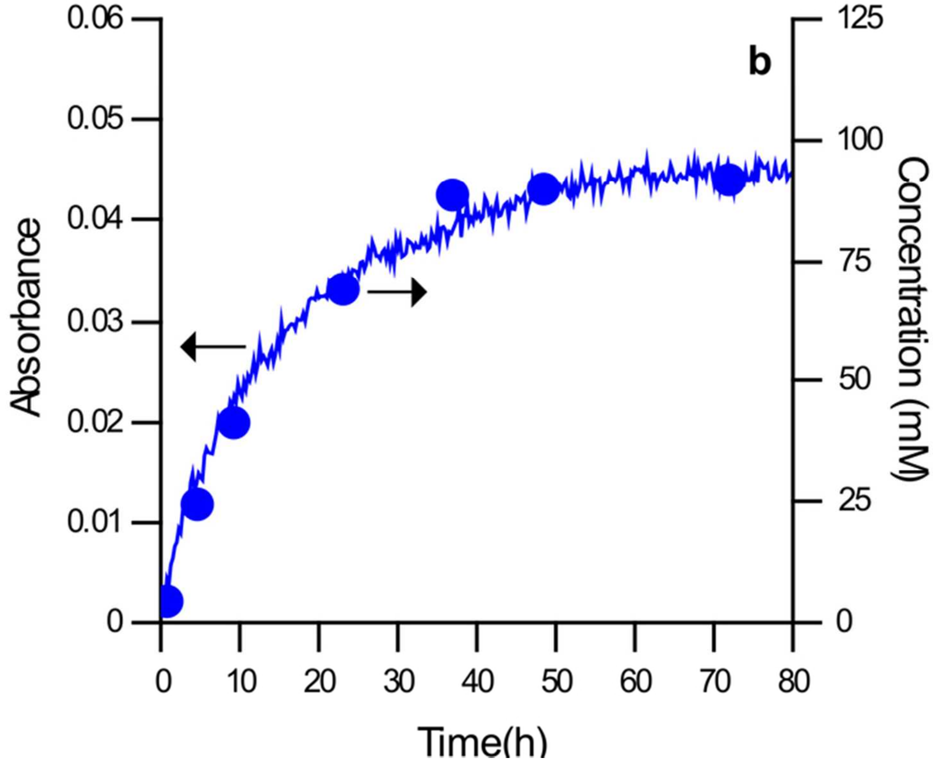


Figure 3b
66x51mm (300 x 300 DPI)

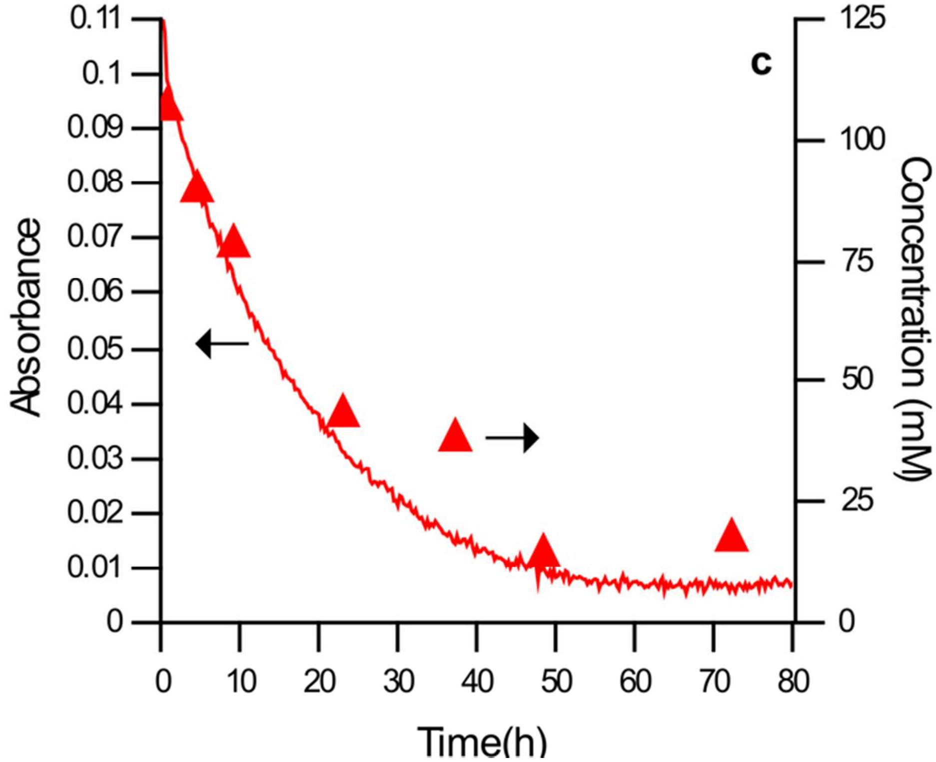


Figurer 3c
66x51mm (300 x 300 DPI)

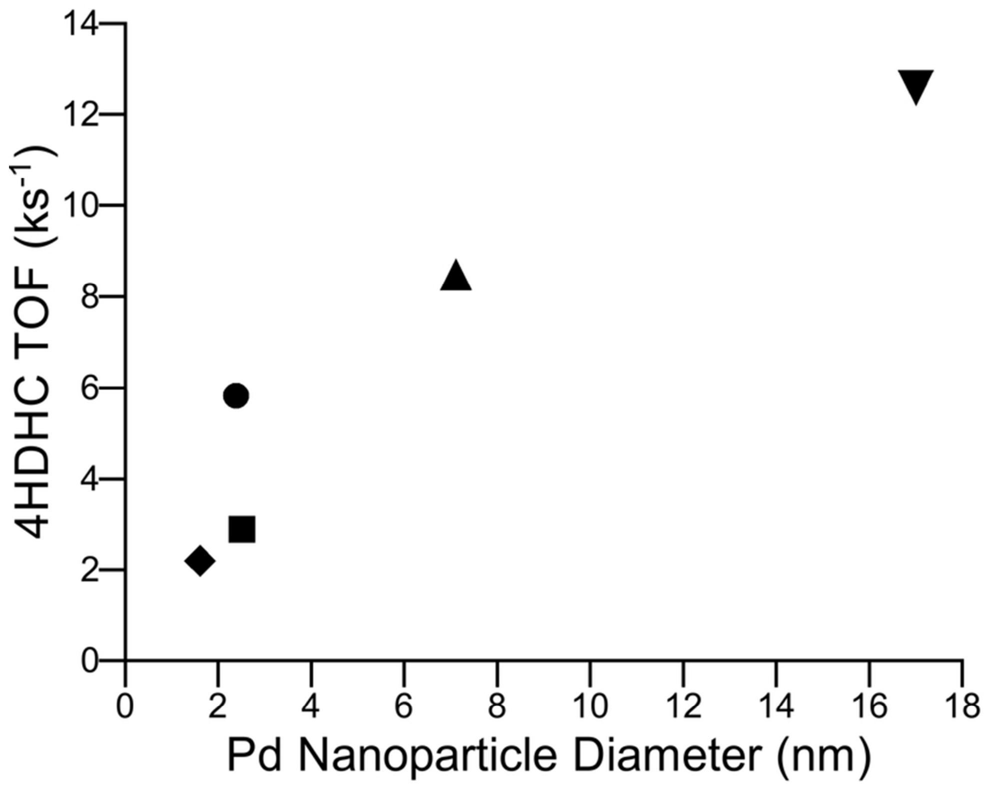


Figure 4
73x61mm (300 x 300 DPI)

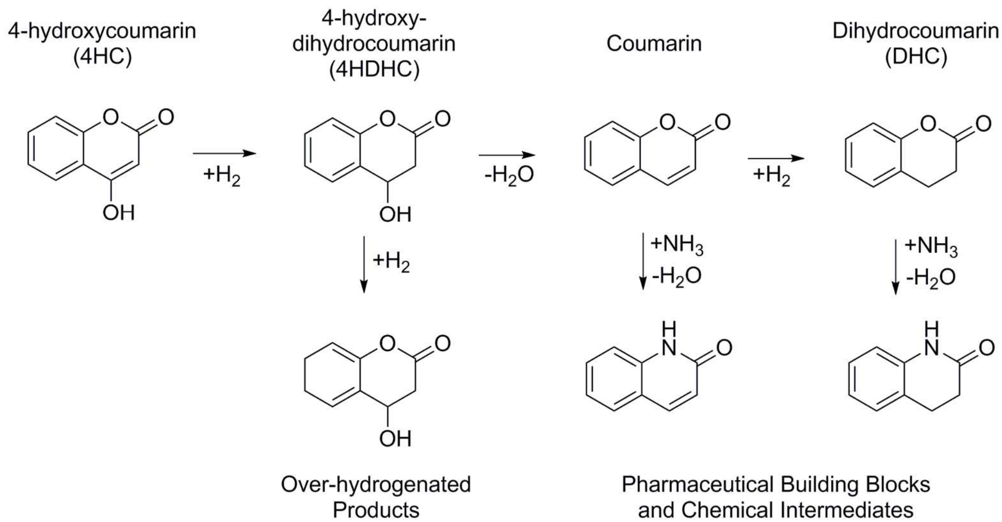


Scheme 1
159x83mm (300 x 300 DPI)